

EEGDM: Learning EEG Representation with Latent Diffusion Model

Shaocong Wang^{1*}, Tong Liu^{1*}, Ming Li¹, Minjing Yu², Yong-Jin Liu^{1†}

¹Department of Computer Science and Technology, Tsinghua University

²College of Intelligence and Computing, Tianjin University

{wangsc23, tongliu, mingli_thu, liuyongjin}@tsinghua.edu.cn,
minjingyu@tju.edu.cn

Abstract

While electroencephalography (EEG) signal analysis using deep learning has shown great promise, existing approaches still face significant challenges in learning generalizable representations that perform well across diverse tasks, particularly when training data is limited. Current EEG representation learning methods including EEGPT and LaBraM typically rely on simple masked reconstruction objective, which may not fully capture the rich semantic information and complex patterns inherent in EEG signals. In this paper, we propose EEGDM, a novel self-supervised EEG representation learning method based on the latent diffusion model, which leverages EEG signal generation as a self-supervised objective, turning the diffusion model into a strong representation learner capable of capturing EEG semantics. EEGDM incorporates an EEG encoder that distills EEG signals and their channel augmentations into a compact representation, acting as conditional information to guide the diffusion model for generating EEG signals. This design endows EEGDM with a compact latent space, which not only offers ample control over the generative process but also can be leveraged for downstream tasks. Experimental results show that EEGDM (1) can reconstruct high-quality EEG signals, (2) effectively learns robust representations, and (3) achieves competitive performance with modest pre-training data size across diverse downstream tasks, underscoring its generalizability and practical utility.

Introduction

Electroencephalography (EEG) is a non-invasive technique that measures spontaneous electrical activity in the brain through scalp electrodes. The interpretation and utilization of EEG signals generally require sophisticated signal processing pipelines and advanced feature extraction methodologies (Mohsenvand et al. 2020). Conventional EEG signal analysis typically employs manually engineered operations tailored to specific EEG features of interest (e.g., band-pass filtering in a specific frequency range), potentially excluding other informative signal components (Zander and Kothe 2011).

Recently, deep learning has introduced a new research paradigm for EEG signal analysis due to its capability to automatically learn efficient representations from original data (Zhao, Yan, and Lu 2021; Zheng et al. 2023; Chen et al.

2025). Current deep learning-based approaches, which predominantly rely on large-scale EEG datasets, can be broadly classified into two categories: (1) task-specific models, and (2) multi-task large models. Task-specific models face significant challenges in generalization due to substantial variations across datasets in channel configurations, sampling rates, and EEG recording time lengths. These discrepancies necessitate model training on individual datasets, thereby severely limiting cross-dataset generalizability. For multiple tasks, two large EEG models, EEGPT (Wang et al. 2024) and LaBraM (Jiang, Zhao, and Lu 2024) have recently been proposed. Both models learn generic representations through masked reconstruction pre-training objective before being fine-tuned for various downstream tasks. However, LaBraM uses a substantially larger dataset, and EEGPT’s performance across diverse specific tasks still leaves room for improvement.

In this paper, we introduce the Diffusion Model (DM) (Ho, Jain, and Abbeel 2020; Dhariwal and Nichol 2021) into EEG representation learning and propose a novel self-supervised framework called EEGDM. Our framework leverages EEG signal synthesis as a self-supervised objective, turning the diffusion model into a strong representation learner capable of capturing EEG semantics. Unlike popular masked reconstruction approaches that primarily focus on local feature recovery, DM learns effective representations through a self-supervised denoising objective that requires understanding the underlying data distribution. This makes DM potentially valuable for generic EEG representation learning. Building on this observation, our framework uses an EEG encoder that transforms input signals and their channel augmentations into compact latent representations, which condition the diffusion process. This design enables the encoder to learn the effective and generic representations inherent in EEG signals that are crucial for downstream tasks.

We note that EEG signals present unique challenges due to their inherently low signal-to-noise ratio (SNR) and complex characteristics, including stochasticity, nonstationarity, and nonlinearity (Gramfort et al. 2013; Cole and Voytek 2019). To address these challenges, we incorporate two key technical components in our EEGDM framework. First, we employ channel augmentation that provides diverse training perspectives while enriching the conditional information. Second, we utilize Principal Component Analysis (PCA) to project EEG signals into a latent space with an improved SNR, as

*These authors contributed equally.

†Corresponding author.

it enhances signal-relevant components while suppressing noise-related ones (Sanei and Chambers 2013). This transformation mitigates the challenge of reconstructing the original noisy signal. Inspired by the success of state-of-the-art DMs (e.g., Latent Diffusion Models (LDMs) (Rombach et al. 2022) and Diffusion Transformers (DiTs) (Peebles and Xie 2023)) operating in latent spaces, we apply our DM to this PCA-derived latent space rather than the original noisy EEG space. This enables EEGDM to focus on learning meaningful signal patterns for effective representation learning across diverse downstream tasks. Our experiments show that EEGDM effectively learns robust representations, achieving competitive performance across diverse downstream tasks with modest pre-training data requirements and exhibiting strong generalizability.

Our contributions are summarized as follows:

- We propose EEGDM, a novel diffusion model-based self-supervised framework for EEG representation learning. By leveraging EEG signal generation as the self-supervised objective, EEGDM transforms the diffusion model into a powerful representation learner that captures rich EEG semantics, even with limited pre-training data.
- EEGDM incorporates channel augmentation and elaborately designed PCA-based latent space operations to (1) enhance the conditional information available for DM, (2) enable robust EEG signal reconstruction, and (3) improve the cross-dataset generalizability of learned EEG representations.
- We validate the effectiveness and generalizability of EEGDM across multiple EEG analysis tasks, demonstrating its (a) competitive performance compared to existing methods and (b) strong cross-dataset transferability and practical utility in EEG applications.

Related Work

Self-supervised EEG Representation Learning

Self-supervised learning can leverage large amounts of unlabeled data for pre-training, thereby reducing the reliance on manual annotations. This methodology has led to significant breakthroughs in natural language processing and computer vision (Kenton and Toutanova 2019; He et al. 2022). However, its full potential in EEG analysis remains largely unexplored (Jiang et al. 2025).

Some studies (Mohsenvand et al. 2020; Banville et al. 2021) have explored learning representations of EEG signals via contrastive learning, which trains a channel feature extractor by extending the SimCLR framework (Chen et al. 2020) to time series data. Another line of work extends the mask idea to EEG analysis (Mohammadi Foumani et al. 2024). For instance, BENDR (Kostas et al. 2021) uses a convolutional encoder to extract EEG features from local time windows, masks a portion of them, and utilizes a Transformer to predict the information in the masked part. LaBraM (Jiang, Zhao, and Lu 2024) pre-trains a Transformer model by predicting the original neural codes of masked EEG channel patches based on a defined neural codebook. EEGPT (Wang et al. 2024) introduces the alignment of spatio-temporal represen-

tation, implemented by a mask-based dual self-supervised learning for efficient extraction of EEG features.

Unlike the above approaches, we explore self-supervised EEG representation learning via generative models. Our proposed EEGDM not only facilitates high-quality EEG generation but also enables the learning of rich and robust representations for downstream tasks.

Diffusion Model

Diffusion models learn complex data distributions through a progressive denoising process that requires a deep understanding of the underlying data structure and semantics. This fundamental characteristic endows them with dual capabilities: generating high-quality samples and learning meaningful representations inherent in the data distribution. The pioneering work by Sohl-Dickstein et al. (Sohl-Dickstein et al. 2015) and subsequent advances by Ho et al. (Ho, Jain, and Abbeel 2020) established diffusion models as powerful tools, leading to widespread applications in generative tasks (Rombach et al. 2022; Peebles and Xie 2023; Zhang, Rao, and Agrawala 2023). More recently, their potential for representation learning has gained attention, with emerging studies showing promising results in learning discriminative features (Mittal et al. 2023; Chen et al. 2024b; Hudson et al. 2024).

In the EEG domain, existing diffusion-based approaches have primarily focused on generative applications, such as EEG synthesis and data augmentation (Huang et al. 2024; Chen et al. 2024a; Huang, Li, and Chen 2025), or a few specific supervised tasks (Kim et al. 2023, 2024). However, the potential of diffusion models for generic EEG representation learning remains largely unexplored. This presents a significant opportunity, as learning the complex temporal and spatial characteristics of EEG signals can benefit from the understanding of rich data distributions inherent in diffusion models' denoising process. In this paper, we present a novel method that exploits the representational capacity of diffusion models for self-supervised EEG representation learning.

Method

Our study is motivated by the following observation: Diffusion models capable of generating rich and high-fidelity content from scratch are likely to effectively characterize the underlying properties, structures, and dynamics of the data during the generative process. Therefore, we explore self-supervised EEG representation learning via the diffusion model, and design the following framework architecture.

Framework Architecture

Our proposed self-supervised EEG representation learning framework, EEGDM, is formulated as a latent diffusion model (DM) conditioned on EEG channel augmentation. Our goal is to generate high-quality EEG signals while equipping the model with a generalizable understanding of EEG data that can be effectively adapted to various downstream tasks. It is worth noting that in the denoising process of DM, directly reconstructing raw EEG signals is challenging due to their inherently low SNR. To address this, we utilize PCA

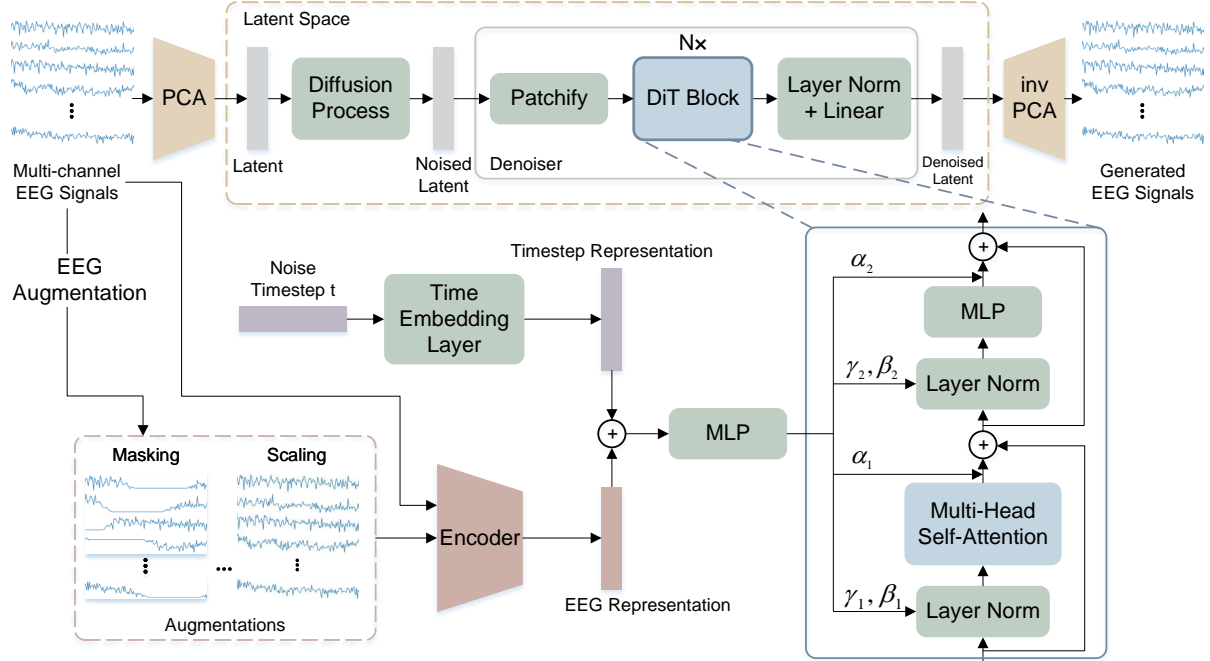


Figure 1: The overall architecture of EEGDM. The original EEG data is projected onto a latent space using PCA. Noise is added in this latent space, and the denoised latent representation is predicted by learning the conditional latent diffusion model. The prediction is then projected back to the original space by inverse PCA to obtain the generated target EEG signal. The encoder transforms the source EEG signal (including original data and augmentations) into a concise EEG representation. It is combined with the noise timestep representation and then used as conditional information to modulate the DiT block, thus guiding the denoising of the latent representation.

to preprocess the original EEG for noise reduction, and perform the reconstruction on the preprocessed EEG data with a relatively high SNR. The overall architecture of EEGDM is illustrated in Figure 1.

Specifically, given the original multi-channel EEG signals $X \in \mathbb{R}^{C \times T}$, where C is the number of EEG electrodes (channels) and T is the total timestamp, we segment X into $\lfloor \frac{T-t^s}{s^t} \rfloor + 1$ samples. This segmentation assumes a timestamp length¹ t^s per sample and a stride s^t . As shown in Figure 1, each multi-channel sample $x \in \mathbb{R}^{C \times t^s}$ is processed by PCA to obtain the latent representation z . Our diffusion model operates on this latent space, where noise is added and predicted. The denoised latent representation predicted by the diffusion model is projected back to the original space by inverse PCA to obtain the target EEG signal. Owing to the effectiveness of the DiT model in the latent space, we utilize it to predict the denoised latent representations. Furthermore, we introduce an EEG encoder that transforms the input source signal x' (including original EEG sample and its augmentations) into an EEG representation containing rich semantic information. The sum of this EEG representation and the noise timestep representation (i.e., timestep t in the noise-adding

process) encoded by the time embedding layer serves as the conditional input information for the diffusion model. This diffusion model design can utilize the semantically rich external EEG representation for the generative task, leading to a significant improvement in generative performance. Consequently, this enhances the model's representation learning capability.

The EEG Encoder

The representation output from the EEG encoder lies at the core of EEGDM, which (1) acts as the communication bridge between the encoder and the denoiser (ϵ_θ), and (2) guides the denoising process. In more details, this output represents a clean source EEG signal semantically related to the target EEG data. The introduction of the encoded EEG representation is to enable hidden states of the diffusion model to predict noise-invariant and semantically meaningful EEG representations from noisy inputs, guiding the reconstruction of the target EEG data during the denoising process.

The core motivation behind the above EEG encoder design arises from the inherently under-determined nature of the denoising task. The denoiser tends to exploit any relevant knowledge or informative cues to infer and recover the original data distribution as accurately as possible. This incen-

¹Here superscript is used; subscript is reserved for diffusion formation in subsequent sections.

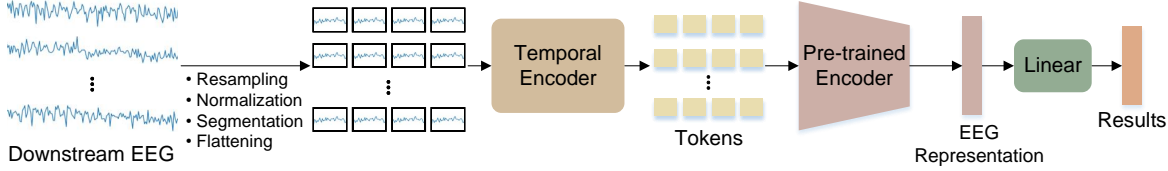


Figure 2: The pre-trained encoder is connected to a linear prediction head to perform downstream tasks.

tivizes the encoder to distill salient commonalities between the source and target EEG signals into a compact representation. We constrain the encoded EEG representation to a low-dimensional latent space and guide the denoiser through feature modulation. This strategy encourages the encoder to capture high-level semantic information in the EEG signals, while leaving the reconstruction of local details to the denoiser. Rather than reconstruction from scratch as most conventional denoisers do (Hinton and Salakhutdinov 2006; Higgins et al. 2017), our strategy enables the encoder to learn a representation that supports latent space denoising. This alleviates the burden of compressing all signal information into the representation, allowing it to prioritize the most distinctive and informative features of the EEG. Such a representation is particularly valuable for adapting to a wide range of downstream EEG tasks.

Our EEG encoder is based on the Vision Transformer (ViT) architecture (Dosovitskiy 2021) that operates on the sequences of tokens. We segment each EEG channel into tokens and then flatten the tokens to form consistent biosignal sequences. We retain many of ViT’s best practices, enabling the EEG encoder to be a Transformer architecture that can process input EEG signals with various formats (different sampling rates, number of channels, and time lengths). The input of the encoder is the source EEG signal x' , which consists of the original samples and the EEG channel augmentations. EEG augmentations are a set of transformations that preserve the semantic information in the EEG channels without altering the interpretation of the EEG data. Here, we employ two augmentations (zero-masking and amplitude scaling) which were shown in prior work (Mohsenvand et al. 2020) to be the most effective for extracting useful features.

Specifically, we use a ω -length window without overlap to segment each EEG channel sample into patches ($x' = \{x'_{j,k} \in \mathbb{R}^\omega | j = 1, 2, \dots, C, k = 1, 2, \dots, \lfloor \frac{t^s}{\omega} \rfloor\}$). The total number of patches for x' is $|x'| = C \lfloor \frac{t^s}{\omega} \rfloor$. Then a temporal encoder (i.e., a temporal convolution block) is used to encode each EEG patch into a patch embedding $e' = \{e'_{j,k} \in \mathbb{R}^d | j = 1, 2, \dots, C, k = 1, 2, \dots, \lfloor \frac{t^s}{\omega} \rfloor\}$, where d is the dimension of the embeddings. The learnable positional embeddings are added to all input patch embeddings. Finally, the sequence of embeddings is fed directly into the Transformer network. We use average pooling on the output embeddings to obtain the EEG representation, which is then combined with the noise timestep representation to guide the denoising of the diffusion model. In addition, we

perform downstream EEG tasks by using task-specific prediction heads on the EEG representation. As shown in Figure 2, we train a linear classifier as the prediction head based on the pre-trained encoder in fine-tuning and then analyze the model’s performance on the downstream tasks, in which we employ cross-entropy loss. The implementation details can be found in the supplementary material.

EEG Data Generation by Diffusion Model

As aforementioned, due to the inherently low SNR of original EEG signals, accurate reconstruction of them directly in the denoising process is challenging. To address this, we first enhance the SNR of the raw EEG signals using PCA. Similar to the LDMs (Rombach et al. 2022), we find a perceptually equivalent yet computationally more suitable space in which the diffusion model is trained for generating high-SNR EEG signals. In addition, we use the high-quality representation from the EEG encoder to guide the diffusion process. After denoising in the latent space, we apply inverse PCA to project the latent EEG representations back to the original signal space, thereby reconstructing the final EEG signals.

Diffusion Formulation The input to our proposed latent diffusion model, which is conditioned on channel augmentation, is the latent representation $z = Px$ obtained through PCA pre-processing. Here, we use the ω -length window to segment each x before applying PCA to obtain the corresponding latent representation. The PCA basis vectors are computed via eigen-decomposition without the need for gradient-based training. Our diffusion model operates within this latent space. The noisy input z_t at a given timestep is transformed into patches, which are then linearly embedded into a sequence of tokens with dimension d (implemented by the patchify layer). Here, we apply a sine-cosine version of the positional embeddings to all input tokens. Then, the input tokens are processed by several DiT blocks. By applying the reparameterization trick, we can do the sampling as follows:

$$z_t = \sqrt{\bar{\alpha}_t} z_0 + \sqrt{1 - \bar{\alpha}_t} \epsilon_t, \quad (1)$$

where $\epsilon_t \sim \mathcal{N}(0, \mathbf{I})$. The diffusion model is trained to learn the reverse denoising process:

$$p_\theta(z_{t-1}|z_t) = \mathcal{N}(\mu_\theta(z_t), \Sigma_\theta(z_t)), \quad (2)$$

where the network is used to predict the statistics of p_θ . By reparameterizing μ_θ as a noise prediction network (i.e., denoiser) ϵ_θ , the model can be trained using the mean squared

error between the predicted noise $\epsilon_\theta(z_t)$ and the ground truth sampled Gaussian noise ϵ_t :

$$\mathcal{L}_{simple}(\theta) = \|\epsilon_\theta(z_t) - \epsilon_t\|_2^2. \quad (3)$$

To train the diffusion model with a learned reverse process covariance Σ_θ , we follow the approach of Nichol et al. (2021): train ϵ_θ with \mathcal{L}_{simple} and train Σ_θ with \mathcal{L}_{vlb} . After the final DiT block, we use a standard linear decoder to decode the token sequence into an output noise prediction and an output diagonal covariance prediction. Both outputs have the same data shape as the input. Once p_θ is trained, new latent representations can be sampled by initializing $z_{t_{max}} \sim \mathcal{N}(0, \mathbf{I})$ and sampling $z_{t-1} \sim p_\theta(z_{t-1}|z_t)$ via the reparameterization trick. Finally, we obtain the denoised latent representation \tilde{z} , which is then projected back to the original signal space using inverse PCA to reconstruct the original EEG signals:

$$\tilde{x} = P^{-1}\tilde{z} = P^T\tilde{z}. \quad (4)$$

Conditional Guidance We incorporate the encoded EEG representation as conditional input for the diffusion model. It guides the generative process and is further leveraged for downstream tasks. To this end, we broadly consider EEG signals in this context as any collection of EEG recordings that exhibit meaningful interrelationships (e.g., semantic correlations), particularly those derived through various augmentations of source EEG signals — an approach well-established in contrastive learning frameworks (Chen et al., 2020). Specifically, each augmented EEG signal is encoded using a shared EEG encoder, and the resulting EEG representations $e^{1:m}$ are aggregated into a single vector e by taking their mean, enabling the model to incorporate richer conditional information. When the conditional input is e , the reverse process of the diffusion model is $p_\theta(z_{t-1}|z_t, e)$, where both ϵ_θ and Σ_θ are conditioned on e . Under this setting, classifier-free guidance (Ho and Salimans 2022) can be applied to encourage the sampling process to find z such that $\log p(e|z)$ is maximized. According to Bayes’ rule, $p(e|z) \propto p(z|e)/p(z)$, and thus $\nabla_z \log p(e|z) \propto \nabla_z \log p(z|e) - \nabla_z \log p(z)$. By interpreting the output of the diffusion model as a score function, the sampling process can be guided by:

$$\begin{aligned} \tilde{\epsilon}_\theta(z_t, e) &\propto \epsilon_\theta(z_t, \emptyset) + s \cdot (\epsilon_\theta(z_t, e) - \epsilon_\theta(z_t, \emptyset)), \\ \tilde{\epsilon}_\theta(z_t, e) &= \epsilon_\theta(z_t, \emptyset) + s \cdot (\nabla_z \log p(z|e)), \end{aligned} \quad (5)$$

where $s > 1$ denotes the scale of the guidance. The diffusion model with $e = \emptyset$ is trained by randomly dropping e during training and replacing it with a learned null embedding \emptyset . The classifier-free guidance sampling method can significantly improve the quality of generated samples by effectively utilizing the conditional information we introduced.

Conditional Input Setup The treatment of conditional inputs and the initialization process significantly influence the generation quality in diffusion models. We adopt the adaLN-Zero block from DiT, which has shown superior performance, to handle the conditional inputs (the EEG representations e and the noise timestep t). Specifically, we regress the scale and shift parameters γ and β in the Transformer blocks based on the sum of the e and t . Additionally, we regress the dimension-wise scaling parameters α , which

are applied just before each residual connection in the DiT blocks. The MLP for all α is initialized to output the zero vector, which effectively initializes the entire DiT block as an identity function. In addition to layer normalization, we incorporate conditional embeddings into residual connections, which enhance the vanilla adaLN and improve the quality of the generated EEG signals.

Experiments

Datasets

Pre-training datasets. We pre-train the proposed EEGDM on several publicly available EEG datasets covering a range of paradigms, including **PhysioMI** (motor imagery and execution dataset) (Goldberger et al. 2000), **TSU** (steady-state visual evoked potential dataset) (Wang et al. 2016), **SEED** (emotion recognition dataset) (Zheng and Lu 2015), and **M3CV** (multi-subject multi-session multi-paradigm dataset) (Huang et al. 2022).

Datasets of downstream specific tasks. (1) **TUAB** (abnormal detection) (Obeid and Picone 2016): A corpus of EEG recordings annotated as either normal or abnormal. (2) **TUEV** (event type classification) (Obeid and Picone 2016): An EEG dataset containing six event categories: spike and sharp wave (SPSW), generalized periodic epileptiform discharges (GPED), periodic lateralized epileptiform discharges (PLED), eye movement (EYEM), artifact (ARTF), and background (BCKG). (3) **BCIC-2A** (motor imagery classification) (Tangermann et al. 2012): A four-class motor imagery dataset comprising left hand, right hand, feet, and tongue movement imagination tasks. (4) **BCIC-2B** (motor imagery classification) (Steyrl et al. 2016): A binary motor imagery dataset containing left-hand and right-hand movement imagination tasks.

Experimental Setup

We evaluate EEGDM’s representation learning capabilities through fine-tuning on downstream tasks. Following previous work (Wang et al. 2024), we adopt standard preprocessing procedures including resampling, normalization, segmentation, and flattening. For TUAB and TUEV datasets, we use the provided train-test splits, while BCIC-2A and BCIC-2B employ Leave-One-Subject-Out (LOSO) cross-validation. The reported model sizes correspond to the downstream networks used for fine-tuning, as the generative modules are not involved in downstream tasks. We compare with state-of-the-art baselines and provide results for both EEGDM (25M parameters) and a compact variant, EEGDM-Tiny (3M parameters), which uses a smaller pre-training architecture. Detailed configurations for both model variants are provided in the supplementary material. Complete implementation details and hyperparameters for both pre-training and fine-tuning are also provided in the supplementary material.

Results and Analysis

In this section, we show that EEGDM achieves competitive performance across diverse downstream tasks, demonstrating the effectiveness of diffusion-based representation learning

Methods	Model Size	Balanced Accuracy \uparrow	AUROC \uparrow
ST-Transformer (Song et al. 2021)	3.5M	0.7966 \pm 0.0023	0.8707 \pm 0.0019
CNN-Transformer (Peh, Yao, and Dauwels 2022)	3.2M	0.7777 \pm 0.0022	0.8461 \pm 0.0013
SPaRCNet (Jing et al. 2023)	0.79M	0.7896 \pm 0.0018	0.8676 \pm 0.0012
BIOT (Yang, Westover, and Sun 2024)	3.2M	0.7959 \pm 0.0057	0.8815\pm0.0043
LaBraM (Jiang, Zhao, and Lu 2024)	9.4M	0.7964 \pm 0.0120	0.8749 \pm 0.0047
EEGPT (Wang et al. 2024)	25M	<u>0.7983\pm0.0030</u>	0.8718 \pm 0.0050
EEGDM-Tiny	3.3M	0.7885 \pm 0.0037	0.8690 \pm 0.0032
EEGDM	25M	0.8017\pm0.0030	0.8739 \pm 0.0026

Table 1: Performance comparison on TUAB. The best metric is highlighted in bold, and the second-best metric is underlined.

Methods	Model Size	Balanced Accuracy \uparrow	Weighted F1 \uparrow	Cohen’s Kappa \uparrow
ST-Transformer (Song et al. 2021)	3.5M	0.3984 \pm 0.0228	0.6823 \pm 0.0190	0.3765 \pm 0.0306
CNN-Transformer (Peh, Yao, and Dauwels 2022)	3.2M	0.4087 \pm 0.0161	0.6854 \pm 0.0293	0.3815 \pm 0.0134
SPaRCNet (Jing et al. 2023)	0.79M	0.4161 \pm 0.0262	0.7024 \pm 0.0104	0.4233 \pm 0.0181
BIOT (Yang, Westover, and Sun 2024)	3.2M	0.5281 \pm 0.0225	<u>0.7492\pm0.0082</u>	0.5273 \pm 0.0249
LaBraM (Jiang, Zhao, and Lu 2024)	9.4M	0.5768 \pm 0.0088	0.7457 \pm 0.0250	0.5287 \pm 0.0427
EEGPT (Wang et al. 2024)	25M	0.6232\pm0.0114	0.8187\pm0.0063	0.6351\pm0.0134
EEGDM-Tiny	3.3M	0.5700 \pm 0.0034	0.6840 \pm 0.0172	0.4223 \pm 0.0210
EEGDM	25M	<u>0.6081\pm0.0011</u>	0.7430 \pm 0.0239	0.5218 \pm 0.0355

Table 2: Performance comparison on TUEV. The best metric is highlighted in bold, and the second-best metric is underlined.

for EEG analysis. All experiments are conducted with three random seeds, and we report mean and standard deviation values as shown in Tables 1, 2, and 3. Additional results under different fine-tuning settings are provided in the supplementary material.

On the TUAB dataset, EEGDM achieves a balanced accuracy of 80.17%, outperforming both the previous state-of-the-art method EEGPT (79.83%) and other baselines. The AUROC score of 87.39% further demonstrates strong discriminative capability. For TUEV classification, EEGDM obtains 60.81% balanced accuracy with a Cohen’s Kappa coefficient 0.5218, achieving either (1) good balance between performance and pre-training data size, when compared to EEGPT, or (2) substantial improvements over other baselines. On motor imagery classification, EEGDM shows competitive performance, achieving 55.95% balanced accuracy on BCIC-2A and 72.19% on BCIC-2B, with the latter outperforming both EEGPT and LaBraM.

Regarding the comparison with EEGPT and LaBraM, the following detailed explanations are necessary. Following EEGPT (Wang et al. 2024), all comparisons are conducted with LaBraM-Base (Jiang, Zhao, and Lu 2024). The LaBraM results are based on the same pre-training dataset as ours, rather than their original larger dataset (which includes TUEG dataset, whose distribution is similar to the TUAB and TUEV). Remarkably, our EEGDM achieves performance comparable to or better than EEGPT despite using a smaller pre-training dataset. Even our compact EEGDM-Tiny model maintains competitive performance while using substantially fewer parameters. These results validate the effectiveness of using EEG signal generation as a self-supervised pre-training

objective, demonstrating that the combination of encoder and diffusion denoiser, enhanced by PCA and channel augmentation, successfully learns high-quality EEG representations for improved downstream task performance.

Ablation Study We conduct ablation studies to analyze the contributions of PCA and channel augmentation components, respectively, by setting up four variant versions as shown in Table 4, in which the average balanced accuracy on three random seeds is reported. For BCIC-2A and BCIC-2B, we report the results using the LOSO evaluation protocol. Variant D consistently achieves the best performance across all settings, demonstrating that both PCA and EEG augmentation are important for our model. Furthermore, for TUAB and TUEV, we randomly selected 10% of the training set for fine-tuning and tested it on the entire test set (see the last two columns in Table 4); we also use this setting in Figure 3. The results show that the advantages of incorporating PCA and EEG augmentation remain evident even when small-scale datasets are used for fine-tuning.

We also investigate the impact of the number of PCA components on downstream task performance. Figure 3 presents results on TUEV and BCIC-2B with varying numbers of PCA components, which reveal a nonlinear relationship between the number of PCA components and downstream task performance. In particular, insufficient number of components may result in large information loss, whereas an excessive number introduces noise contamination, both of which degrade model performance. To balance these trade-offs, we empirically select an intermediate value of 20 components, which yields optimal performance in our experiments.

To evaluate generation quality, we use the diffusion model

Datasets	Methods	Balanced Accuracy \uparrow	Cohen's Kappa \uparrow	Weighted F1 / AUROC \uparrow
BCIC-2A	LaBraM (Jiang, Zhao, and Lu 2024)	<u>0.5784\pm0.0088</u>	0.4378 \pm 0.0118	0.5628 \pm 0.0092
	EEGPT (Wang et al. 2024)	0.5846\pm0.0070	0.4462\pm0.0094	0.5715\pm0.0051
	EEGDM	0.5595 \pm 0.0039	0.4126 \pm 0.0052	0.5580 \pm 0.0051
BCIC-2B	LaBraM (Jiang, Zhao, and Lu 2024)	0.6963 \pm 0.0005	0.3925 \pm 0.0010	0.7650 \pm 0.0027
	EEGPT (Wang et al. 2024)	0.7212 \pm 0.0019	0.4426 \pm 0.0037	0.8059\pm0.0032
	EEGDM	0.7219\pm0.0028	0.4439\pm0.0057	0.7962 \pm 0.0037

Table 3: Performance comparison on BCIC. The best metric is highlighted in bold, and the second-best metric is underlined.

Variants	PCA	EEG Augmentation	BCIC-2A \uparrow	BCIC-2B \uparrow	TUAB (10%) \uparrow	TUEV (10%) \uparrow
A	\times	\times	0.4941 \pm 0.0043	0.7097 \pm 0.0024	0.7755 \pm 0.0071	0.5174 \pm 0.0066
B	\checkmark	\times	0.5159 \pm 0.0062	0.7149 \pm 0.0056	0.7781 \pm 0.0068	0.5479 \pm 0.0097
C	\times	\checkmark	0.5144 \pm 0.0117	0.7148 \pm 0.0037	0.7844 \pm 0.0038	0.5549 \pm 0.0123
D	\checkmark	\checkmark	0.5595 \pm 0.0039	0.7219 \pm 0.0028	0.7858 \pm 0.0006	0.5802 \pm 0.0058

Table 4: The results of the ablation studies for PCA and EEG augmentation, using the metric of average balanced accuracy.

in EEGDM under the same pre-training configuration, and compute Pearson correlation coefficients between the generated and original signals in both time and frequency domains. When PCA is applied, the correlation coefficients improve significantly to 0.36 (time domain) and 0.88 (frequency domain), compared to lower values of 0.003 and 0.83 without PCA. These results demonstrate that integrating PCA substantially improves the quality of EEG data generation, which further facilitates better representation learning.

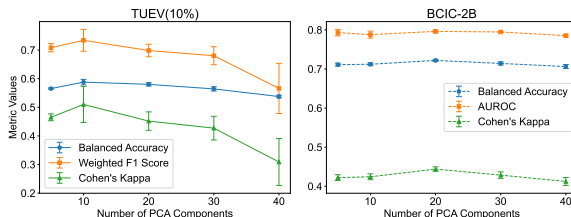


Figure 3: Performance comparison with different numbers of PCA components on TUEV and BCIC-2B datasets.

Visualization To evaluate the quality of learned representations, we visualize the EEG data embeddings using t-SNE (Van der Maaten and Hinton 2008) as presented in Figure 4. We randomly sample EEG signals from the test sets of four downstream tasks in a class-balanced manner and extract their representations using our pre-trained encoder. The t-SNE visualizations exhibit well-separated clusters across all datasets, indicating that our EEGDM learns discriminative representations capable of capturing task-relevant patterns. This clear clustering structure further demonstrates the EEGDM’s ability to learn generic yet informative EEG representations that can be successfully adapted to diverse downstream tasks. Beyond representation learning, EEGDM also achieves high-quality EEG signal reconstruction, as evidenced by visualizations of reconstructed signals and their power spectral density (PSD) analyses provided in the sup-

plementary material.

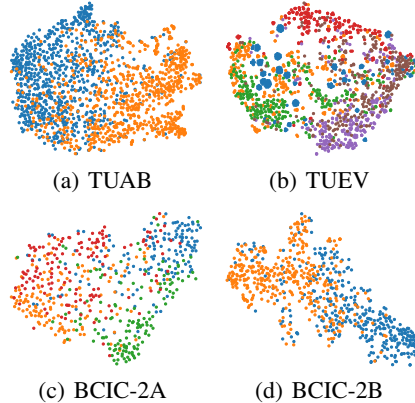


Figure 4: The t-SNE visualizations. Clear inter-class separation and intra-class compactness indicate that the learned representations are discriminative.

In summary, our experimental results highlight three key advantages of EEGDM: (1) *High-quality EEG reconstruction*, as validated by the visualizations in supplementary material; (2) *Effective representation learning*, evidenced by distinct class separation in t-SNE visualizations and consistent performance improvements across tasks; (3) *Competitive performance* across diverse downstream tasks using modest pre-training data sizes, particularly given that EEGDM matches or exceeds EEGPT’s performance while using smaller pre-training datasets.

Conclusion

We present EEGDM, a novel latent diffusion framework for EEG representation learning, through explicit conditioning on EEG channel augmentation. Our EEGDM takes the generative task as the self-supervised EEG representation learning

objective. By (1) integrating a denoiser with the EEG encoder and (2) making use of PCA-based projection and EEG channel augmentation, EEGDM can perform the generation task in the latent space using rich conditional information while learning powerful EEG semantic representations that can be applied to diverse downstream tasks. Comprehensive experimental results demonstrate the model's effectiveness across multiple downstream tasks.

References

Banville, H.; Chehab, O.; Hyvärinen, A.; Engemann, D.-A.; and Gramfort, A. 2021. Uncovering the structure of clinical EEG signals with self-supervised learning. *Journal of Neural Engineering*, 18(4): 046020.

Chen, M.; Gui, Y.; Su, Y.; Zhu, Y.; Luo, G.; and Yang, Y. 2024a. Improving EEG Classification Through Randomly Reassembling Original and Generated Data with Transformer-based Diffusion Models. *arXiv*.

Chen, T.; Kornblith, S.; Norouzi, M.; and Hinton, G. 2020. A simple framework for contrastive learning of visual representations. In *ICML*, 1597–1607.

Chen, X.; Liu, Z.; Xie, S.; and He, K. 2024b. Deconstructing denoising diffusion models for self-supervised learning. *arXiv preprint arXiv:2401.14404*.

Chen, Z.; Matsubara, Y.; Sakurai, Y.; and Sun, J. 2025. Long-term eeg partitioning for seizure onset detection. In *AAAI*, volume 39, 14221–14229.

Cole, S.; and Voytek, B. 2019. Cycle-by-cycle analysis of neural oscillations. *Journal of neurophysiology*, 122(2): 849–861.

Dhariwal, P.; and Nichol, A. 2021. Diffusion models beat gans on image synthesis. *Advances in neural information processing systems*, 34: 8780–8794.

Dosovitskiy, A. 2021. An image is worth 16x16 words: Transformers for image recognition at scale. In *ICLR*.

Goldberger, A. L.; Amaral, L. A.; Glass, L.; Hausdorff, J. M.; Ivanov, P. C.; Mark, R. G.; Mietus, J. E.; Moody, G. B.; Peng, C.-K.; and Stanley, H. E. 2000. PhysioBank, PhysioToolkit, and PhysioNet: components of a new research resource for complex physiologic signals. *circulation*, 101(23): e215–e220.

Gramfort, A.; Strohmeier, D.; Haueisen, J.; Hämäläinen, M. S.; and Kowalski, M. 2013. Time-frequency mixed-norm estimates: Sparse M/EEG imaging with non-stationary source activations. *NeuroImage*, 70: 410–422.

He, K.; Chen, X.; Xie, S.; Li, Y.; Dollár, P.; and Girshick, R. 2022. Masked autoencoders are scalable vision learners. In *CVPR*, 16000–16009.

Higgins, I.; Matthey, L.; Pal, A.; Burgess, C. P.; Glorot, X.; Botvinick, M. M.; Mohamed, S.; and Lerchner, A. 2017. beta-vae: Learning basic visual concepts with a constrained variational framework. In *ICLR*.

Hinton, G. E.; and Salakhutdinov, R. R. 2006. Reducing the dimensionality of data with neural networks. *science*, 313(5786): 504–507.

Ho, J.; Jain, A.; and Abbeel, P. 2020. Denoising diffusion probabilistic models. *Advances in neural information processing systems*, 33: 6840–6851.

Ho, J.; and Salimans, T. 2022. Classifier-free diffusion guidance. *arXiv preprint arXiv:2207.12598*.

Huang, G.; Hu, Z.; Chen, W.; Zhang, S.; Liang, Z.; Li, L.; Zhang, L.; and Zhang, Z. 2022. M3CV: A multi-subject, multi-session, and multi-task database for EEG-based biometrics challenge. *NeuroImage*, 264: 119666.

Huang, J.; Li, M.; and Chen, W. 2025. SAD-VER: A Self-supervised, Diffusion probabilistic model-based data augmentation framework for Visual-stimulus EEG Recognition. *Advanced Engineering Informatics*, 65: 103298.

Huang, X.; Li, C.; Liu, A.; Qian, R.; and Chen, X. 2024. EEGDfus: A Conditional Diffusion Model for Fine-Grained EEG Denoising. *IEEE Journal of Biomedical and Health Informatics*.

Hudson, D. A.; Zoran, D.; Malinowski, M.; Lampinen, A. K.; Jaegle, A.; McClelland, J. L.; Matthey, L.; Hill, F.; and Lerchner, A. 2024. Soda: Bottleneck diffusion models for representation learning. In *CVPR*, 23115–23127.

Jiang, W.-B.; Wang, Y.; Lu, B.-L.; and Li, D. 2025. NeuroLM: A Universal Multi-task Foundation Model for Bridging the Gap between Language and EEG Signals. In *ICLR*.

Jiang, W.-B.; Zhao, L.-M.; and Lu, B.-L. 2024. Large brain model for learning generic representations with tremendous EEG data in BCI. In *ICLR*.

Jing, J.; Ge, W.; Hong, S.; Fernandes, M. B.; Lin, Z.; Yang, C.; An, S.; Struck, A. F.; Herlopian, A.; Karakis, I.; et al. 2023. Development of expert-level classification of seizures and rhythmic and periodic patterns during eeg interpretation. *Neurology*, 100(17): e1750–e1762.

Kenton, J. D. M.-W. C.; and Toutanova, L. K. 2019. Bert: Pre-training of deep bidirectional transformers for language understanding. In *Proceedings of naacl-HLT*, volume 1, 2.

Kim, S.; Lee, S.-H.; Lee, Y.-E.; Lee, J.-W.; Park, J.-H.; Kazanzides, P.; and Lee, S.-W. 2024. Brain-driven representation learning based on diffusion model. In *2024 12th International Winter Conference on Brain-Computer Interface (BCI)*, 1–4.

Kim, S.; Lee, Y.-E.; Lee, S.-H.; and Lee, S.-W. 2023. Diff-E: Diffusion-based learning for decoding imagined speech EEG. *arXiv preprint arXiv:2307.14389*.

Kostas, D.; Aroca-Ouellette, S.; Rudzicz, F.; and Rudzicz, F. 2021. BENDR: Using transformers and a contrastive self-supervised learning task to learn from massive amounts of EEG data. *Frontiers in Human Neuroscience*, 15: 653659.

Mittal, S.; Abstreiter, K.; Bauer, S.; Schölkopf, B.; and Mehrjou, A. 2023. Diffusion based representation learning. In *ICML*, 24963–24982.

Mohammadi Foumani, N.; Mackellar, G.; Ghane, S.; Irtza, S.; Nguyen, N.; and Salehi, M. 2024. Eeg2rep: enhancing self-supervised EEG representation through informative masked inputs. In *SIGKDD*, 5544–5555.

Mohsenvand, M. N.; Izadi, M. R.; Maes, P.; and Maes, P. 2020. Contrastive representation learning for electroencephalogram classification. In *Machine Learning for Health*, 238–253.

Nichol, A. Q.; and Dhariwal, P. 2021. Improved denoising diffusion probabilistic models. In *ICML*, 8162–8171.

Obeid, I.; and Picone, J. 2016. The temple university hospital EEG data corpus. *Frontiers in neuroscience*, 10: 196.

Peebles, W.; and Xie, S. 2023. Scalable diffusion models with transformers. In *ICCV*, 4195–4205.

Peh, W. Y.; Yao, Y.; and Dauwels, J. 2022. Transformer convolutional neural networks for automated artifact detection in scalp EEG. In *2022 44th Annual International Conference of the IEEE Engineering in Medicine & Biology Society (EMBC)*, 3599–3602.

Rombach, R.; Blattmann, A.; Lorenz, D.; Esser, P.; and Ommer, B. 2022. High-resolution image synthesis with latent diffusion models. In *CVPR*, 10684–10695.

Sanei, S.; and Chambers, J. A. 2013. *EEG signal processing*. John Wiley & Sons.

Sohl-Dickstein, J.; Weiss, E.; Maheswaranathan, N.; and Ganguli, S. 2015. Deep unsupervised learning using nonequilibrium thermodynamics. In *ICML*, 2256–2265.

Song, Y.; Jia, X.; Yang, L.; and Xie, L. 2021. Transformer-based spatial-temporal feature learning for EEG decoding. *arXiv preprint arXiv:2106.11170*.

Steyrl, D.; Scherer, R.; Faller, J.; and Müller-Putz, G. R. 2016. Random forests in non-invasive sensorimotor rhythm brain-computer interfaces: a practical and convenient non-linear classifier. *Biomedical Engineering/Biomedizinische Technik*, 61(1): 77–86.

Tangermann, M.; Müller, K.-R.; Aertsen, A.; Birbaumer, N.; Braun, C.; Brunner, C.; Leeb, R.; Mehring, C.; Miller, K. J.; Müller-Putz, G. R.; et al. 2012. Review of the BCI competition IV. *Frontiers in neuroscience*, 6: 55.

Van der Maaten, L.; and Hinton, G. 2008. Visualizing data using t-SNE. *Journal of machine learning research*, 9(11).

Wang, G.; Liu, W.; He, Y.; Xu, C.; Ma, L.; and Li, H. 2024. EEGPT: Pretrained Transformer for Universal and Reliable Representation of EEG Signals. In *The Thirty-eighth Annual Conference on Neural Information Processing Systems*.

Wang, Y.; Chen, X.; Gao, X.; and Gao, S. 2016. A benchmark dataset for SSVEP-based brain-computer interfaces. *IEEE Transactions on Neural Systems and Rehabilitation Engineering*, 25(10): 1746–1752.

Yang, C.; Westover, M.; and Sun, J. 2024. Biot: Biosignal transformer for cross-data learning in the wild. *Advances in Neural Information Processing Systems*, 36.

Zander, T. O.; and Kothe, C. 2011. Towards passive brain-computer interfaces: applying brain-computer interface technology to human-machine systems in general. *Journal of neural engineering*, 8(2): 025005.

Zhang, L.; Rao, A.; and Agrawala, M. 2023. Adding conditional control to text-to-image diffusion models. In *ICCV*, 3836–3847.

Zhao, L.-M.; Yan, X.; and Lu, B.-L. 2021. Plug-and-play domain adaptation for cross-subject EEG-based emotion recognition. In *AAAI*, volume 35, 863–870.

Zheng, R.; Li, J.; Wang, Y.; Luo, T.; and Yu, Y. 2023. ScatterFormer: locally-invariant scattering transformer for patient-independent multispectral detection of epileptiform discharges. In *AAAI*, volume 37, 148–158.

Zheng, W.-L.; and Lu, B.-L. 2015. Investigating critical frequency bands and channels for EEG-based emotion recognition with deep neural networks. *IEEE Transactions on autonomous mental development*, 7(3): 162–175.